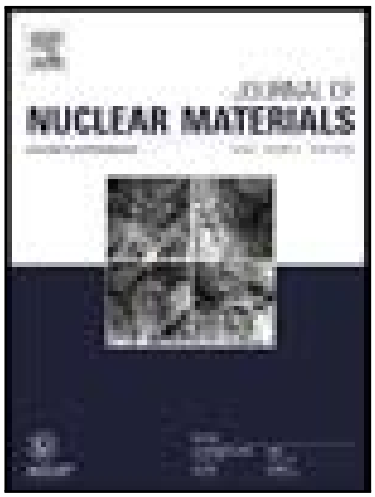

Application of Weibull Fracture Strength Distributions to Modelling Crack Initiation Behaviour in Nuclear Fuel Pellets Using Peridynamics

L.D. Jones , T.A. Haynes , G. Rossiter , M.R. Wenman

PII: S0022-3115(22)00568-2
DOI: https://doi.org/10.1016/j.jnucmat.2022.154087
Reference: NUMA 154087

To appear in: *Journal of Nuclear Materials*

Received date: 20 July 2022
Revised date: 12 October 2022
Accepted date: 12 October 2022

Please cite this article as: L.D. Jones , T.A. Haynes , G. Rossiter , M.R. Wenman , Application of Weibull Fracture Strength Distributions to Modelling Crack Initiation Behaviour in Nuclear Fuel Pellets Using Peridynamics, *Journal of Nuclear Materials* (2022), doi: https://doi.org/10.1016/j.jnucmat.2022.154087

Application of Weibull Fracture Strength Distributions to Modelling Crack Initiation Behaviour in Nuclear Fuel Pellets Using Peridynamics

L.D. Jones[1], T.A. Haynes[2,], G. Rossiter[1] & M.R. Wenman[3]*

[1]National Nuclear Laboratory (NNL), NNL Preston Laboratory, Springfields Works, Salwick, Preston, Lancashire, PR4 0XJ

[2]School of Engineering, University of East Anglia, Norwich Research Park, Norwich, Norfolk, NR4 7TJ

[3]Department of Materials & Centre for Nuclear Engineering,
Imperial College London, Exhibition Road, London, SW7 2AZ

[*]Corresponding author: Dr Thomas Anthony Haynes, Engineering, University of East Anglia, School of Engineering, Faculty of Science University of EaÃ, Norwich, Norfolk NR4 7TJ, United Kingdom, E-mail: t.haynes@uea.ac.uk

Abstract

The thermomechanical behaviour of uranium dioxide nuclear fuel pellets irradiated in a pressurised water reactor has been simulated using a two-dimensional application of bond-based peridynamics implemented in the Abaqus commercial finite element software. Near-surface bond failure, and hence crack initiation, were modelled assuming a probabilistic (variable) failure strain described by a Weibull distribution – with bond failure, and hence crack propagation, in the bulk of the fuel pellets modelled assuming a deterministic (fixed) failure strain. The measured dependency of the number of radial pellet cracks on heat generation rate per unit length – which we show cannot be reproduced by the common assumption in pellet modelling of a deterministic failure strain throughout the pellet volume – was accurately predicted when a size-scaled Weibull distribution with a modulus of 5 was used. However, this low modulus value was associated with the prediction of some cracks initiating away from the pellet surface, which is unphysical. Use of a Weibull modulus of 10 avoided this simulation artefact while still reproducing the experimentally observed dependency with reasonable accuracy.

Keywords

fracture, thermomechanical process, ceramic material,
crack mechanics & peridynamics.

Highlights

- The crack initiation and propagation in UO_2 nuclear fuel pellets has been simulated.
- A 2D application of bond-based peridynamics was implemented in Abaqus.
- Near-surface bond failure strains were calculated using a Weibull distribution.
- Bulk material bond failure strains were set to a constant characteristic value.
- Predictions of pellet cracking behaviour agree well with experimental data.

1 Background

Light water reactors produce the vast majority of the world's nuclear energy. Their fuel commonly consists of cylindrical UO_2 fuel pellets surrounded by a metallic cladding manufactured from a range of zirconium-based alloys. During service, large radial temperature gradients of order 200 K mm-1 are generated in the ceramic fuel pellets, and the resulting differential thermal expansion causes significant thermal stresses. The surface region of the pellet, being closer to the coolant, has a lower temperature, and therefore expands less than the very much hotter centre when at power. This produces tensile hoop stresses in the surface region, and compressive stresses in the centre. These stresses develop to be large enough to cause fracture in the early life of the pellet [1]. Although fracture of the pellet is not a significant issue in itself, upon later life closure of the pellet-clad gap can induce stress in small localised areas of the cladding near crack openings in the pellet. This process can lead to rupture of the clad, a safety issue, for which the umbrella term is pellet-clad interaction (PCI). This issue is currently well mitigated by limiting the operating envelope of the plant [2], or by using liners on the inside of the clad for boiling water reactors [3]. Better understanding of pellet fracture behaviour could allow for alleviating these restrictions, or the development of new PCI resistant fuels.

Peridynamics [4] is a continuum mechanics modelling method that is most useful for modelling brittle fracture. Where traditional continuum mechanics functions on the basis of spatial differential equations, peridynamics is governed by integral equations that are always valid, regardless of the presence of discontinuities. Peridynamics exists in two forms: bond-based peridynamics [4], the original formulation, where material points are connected over finite distances by bonds that exert equal and opposite forces; and state-based peridynamics [5], where the interactions need not be equal and opposite, which offers a wider range of Poisson's ratio and more appropriate modelling of plastic deformation behaviour such as creep [5].

It is common practice in modelling brittle fracture to randomise some aspect of the model since perfectly symmetrical meshes can otherwise tend to fracture in many places at once [6-8]. This randomisation can be in the form of material properties, such as fracture strength, or meshing, such as random perturbation

of mesh nodes. In some cases, [6], both the material properties and mesh are varied. The randomisation is to attempt to better reproduce the observed stochastic aspects of pellet cracking, which include asymmetrical cracking, 'wandering' crack paths and other effects as well as non-simultaneous fracture. This practice has a basis in reality, in that all material fracture, in particular brittle fracture, is governed by flaws and defects, the origins, shapes and sizes of which are so difficult to discern in their entirety that they may be considered randomly distributed. Objects of any engineering size are almost never completely free of flaws, which act as local stress concentrators. In ductile materials, the flaw can be blunted when this stress reaches the yield stress, but for fully brittle materials, this process does not occur, and fracture originates at the tip of these flaws. These flaws originate in events that are, for all intents and purposes, random, so the size of the critical flaw in any object is similarly random, and, following Griffith's fracture criterion [9], so is the fracture strength. It is possible that the critical flaw is almost as large as the object, it is just extremely unlikely.

Weibull distributions, when used for fracture strength, x (usually stress, but often strain or simply load), are defined by three parameters: a modulus, β, defining the degree of variability in the distribution, a characteristic value, x_0, defining the value for for which ~63% of samples would fail at or below, and x_u, the value of x for which the probability of failure, P_f, may be considered to be zero. Since it is often considered true that there is no safe value for strength where failure is considered impossible x_u is often defined as zero, and this form of the Weibull distribution is called a two-parameter Weibull distribution.

Modelling fracture explicitly in nuclear fuel pellets has the potential to offer a great deal of qualitative insight into the process of cracking of in-service fuel. In order for this insight to be useful though, these explicit methods must first be shown to match the quantitative data that exist on fuel pellet crack patterns observed in post-irradiation examination (PIE). Walton and Husser [10] counted radial cracks on low burnup (< 5 GWd tU^{-1}) pressurised water reactor (PWR) pellets after power ramps to various linear heat rates (burnup is the time-integrated power per unit mass).

Barani et al. [11] later fitted a correlation for the number of cracks, N, to the Walton and Husser data using eq. (1), where N_0 is the number of cracks at the

initial cracking event (set to 5 to fit the Walton & Husser data); $\dot{q}'$ is the linear heat rate in kW m^{-1}; $\dot{q}'_0$ is the linear heat rate at the appearance of the first crack (set to 12 to fit the Walton & Husser data); N_∞ is the number of cracks at an arbitrarily high linear heat rate (set to 21 to fit the Walton and Husser data); and τ is a fitting parameter describing the curve.

$$N = 0 \; if \; q' < q'_0 \; N = N_0 + (N_\infty - N_0)\left[1 - exp\left(-\frac{q' - q'_0}{\tau}\right)\right] if \; q' \geq q'_0 \quad (1)$$

The Walton and Husser PIE data are compared in Figure 1 with previously published predictions from three explicit crack modelling simulations of PWR fuel pellets; also included in Figure 1 is the Barani et al. [11] correlation which was fitted to the data. The models of both Huang et al. [6] and Jiang et al. [12] fit the Walton and Husser data remarkably well, given that neither makes reference to it in their work. The agreement with the predictions by Wang et al. [13] is good when only 'longer cracks' are shown.

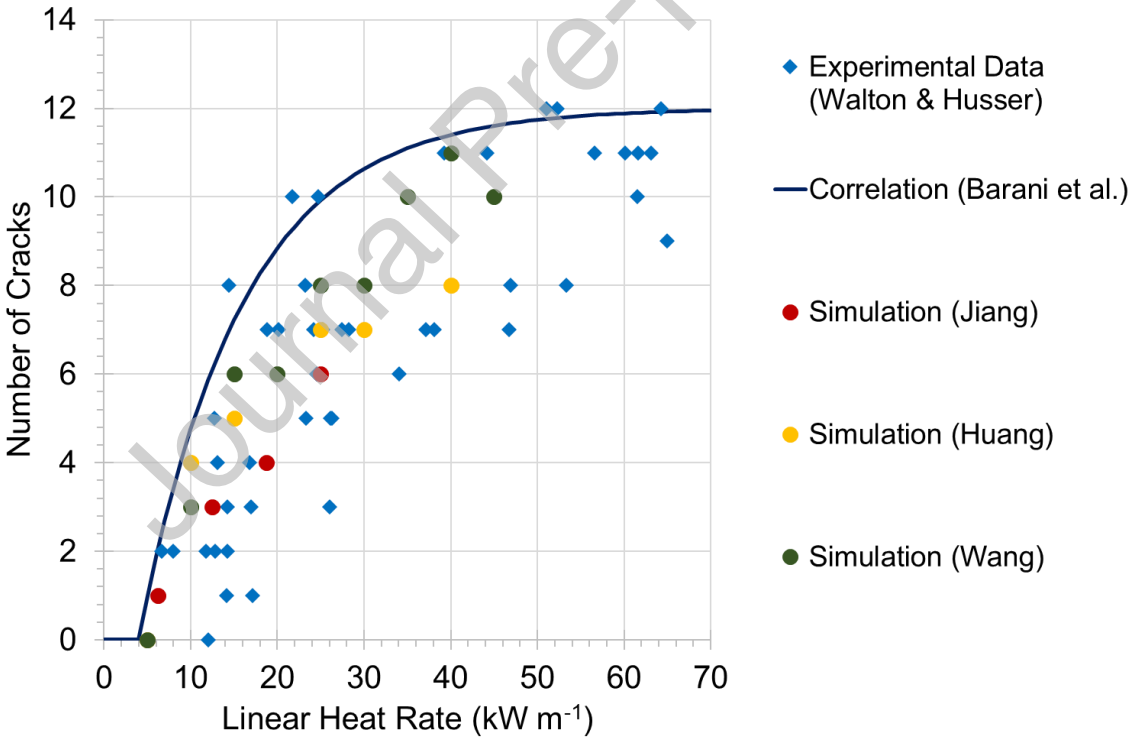

Figure 1 - Radial crack numbers observed in PIE by Walton & Husser [10], and the curve fit to that data by Barani et al. [11] alongside the number of cracks at given linear rate in simulated pellets as modelled by Huang et al. [6], Jiang et al. [12] and Wang et al. [13].

The randomness of fracture strength in brittle materials is represented in a number of different ways in the various explicit nuclear fuel cracking models. In some models it is quite explicitly considered, such as by Oterkus and Madenci [7] who used a Gaussian distribution for failure strain applied to the peridynamics bonds with mean value of 10^{-3} and standard deviation of 10^{-4}, which roughly corresponds to a Weibull distribution with characteristic value 10^{-3} and a Weibull modulus of 10. In other cases, such as the work by Wang et al. [13], no mention is given to this randomness at all, but the crack patterns are not obviously symmetrical, so it may be assumed that some small degree of heterogeneity was used or possibly introduced inadvertently due to numerical rounding in creating the mesh. The degree of randomness is hard to quantify in the discrete element modelling (DEM) model by Huang et al. [6] because in this case it stems from mesh heterogeneity, rather than material properties. That only one result is given suggests that using a different random seed would not materially change the results or it was simply not considered. The phase-field model by Li and Shirvan [8] uses a Weibull distribution of critical fracture stress with parameters of characteristic stress, σ_C = 60 MPa and Weibull modulus, β = 50. It is noted that 60 MPa is around half the value assumed that most models assume for the UO_2 fracture stress [14]. Also of interest is the work by Mella involving lattice site perturbation as a method for introducing heterogeneity sufficient to prevent mesh dependent crack nucleation behaviour [15]. It was found that nodal perturbation did reduce the influence of the mesh on the crack patterns, and did not alter the macroscopic properties of the material. Mella and Wenman found [14] in their LAMMPS implementation of peridynamics that heterogeneity stemming only from rounding errors in the numerical implementation of peridynamics was sufficient to produce a distribution of crack numbers in an advanced gas-cooled reactor pellet similar to PIE data. Similar 3D work was carried out in MOOSE by Hu et al. [16] and offers the possibility of linking to the BISON fuel performance code.

Objects made of typical structural engineering ceramics have Weibull moduli of around 10, with materials such as chalk, brick, stone and pottery having lower values of around 5 [17]. This variation roughly corresponds to that assumed by Oterkus and Madenci [7] for ceramic nuclear fuel pellets, but is significantly greater than the nominal variation in properties used in other explicit pellet

cracking models such as those of Huang et al. [6], Wang et al. [8], or Li and Shirvan [8]. When modelling Weibull distributions, the distribution must be scaled according to the difference in size between the constituent parts of the model (material points in peridynamics) and the engineering scale object in question in order to reproduce Weibull distributions accurately [18, 19]. This can be achieved by increasing the characteristic value, which also increases the difference in the variation of strength between low and high P_f values [20]. Using a distribution of bond strengths, intended to reproduce a real fracture distribution, produces much more variability than the nominal variation typically assumed in fracture modelling.

It is considered here that modelling the simple thermo-mechanical processes is sufficient to get some idea of the reality of initial fuel pellet fracture (i.e. early life behaviour). In order to get a more complete fuel life picture, additional processes must be iteratively added to the model, as Oterkus and Madenci [7], for example, did with oxygen diffusion.

In this paper, it is proposed that the introduction of realistic fracture strength distributions, modelled here as Weibull distributions, are a material property worthy of consideration in accurately reproducing nuclear fuel pellet fracture. A method for appropriately modelling them in a 2D peridynamics approach has been previously outlined by the authors [19]. In this paper, the method is applied to near-surface fracture of ceramic UO_2 nuclear fuel pellets subjected to power ramps to a number of maximum linear heat rates (with fracture in the bulk of the pellets modelled deterministically). The predicted numbers of radial cracks as a function of maximum linear heat rate are compared with both PIE data and the results of previous fracture simulations.

2 Methodology

2.1 Abaqus-Based Peridynamics Implementation

The two-dimensional bond-based implementation of peridynamics in the commercial finite element software Abaqus, was initially presented by Macek and Silling [21]. This implementation has subsequently developed by the authors [19, 22-24] and has recently been extended to model solids with failure described by Weibull statistics [19]. The approach is described in detail

elsewhere [19, 23], and only a brief overview is presented here. Figure 2 shows a 2D section of material decomposed into a series of points, termed 'material points' in peridynamics. The material points represent the material itself and are connected to other material points by linear elastic 'bonds'; these convey forces between the material points. Material points are connected not only to their nearest neighbours, but to all material points within a region known as a 'horizon'. Loads and boundary conditions are applied to the material points and thermal expansion to bonds. When the bonds reach a critical strain, or 'stretch', they fail and no longer convey force. In the Abaqus implementation of peridynamics presented here, the bonds are represented by truss elements and the material points by nodes. Dynamic steps with implicit integration were used. When the trusses reach a critical strain, the bond is broken using the ductile damage model in Abaqus. The damage is therefore included in the equilibrium iteration; this is discussed in more detail elsewhere [19]. The sensitivity of the approach to the mesh and timesteps employed has been discussed previously [24].

A pre-processor written in Fortran and a series of user-defined subroutines for Abaqus are used to for instance:

- construct the mesh of nodes and trusses;
- attach the bonds to nodes using multi-point constraints;
- assign mass to nodes;
- determine the elastic modulus of the truss material so that the elastic response of the peridynamic model is the same as the macroscopic material;
- determine adjustment factors for nodes close to the edge of component to avoid edge effects; and,
- assign the critical strain of the bond according to that that required to capture the overall performance of material using the method developed previously [19].

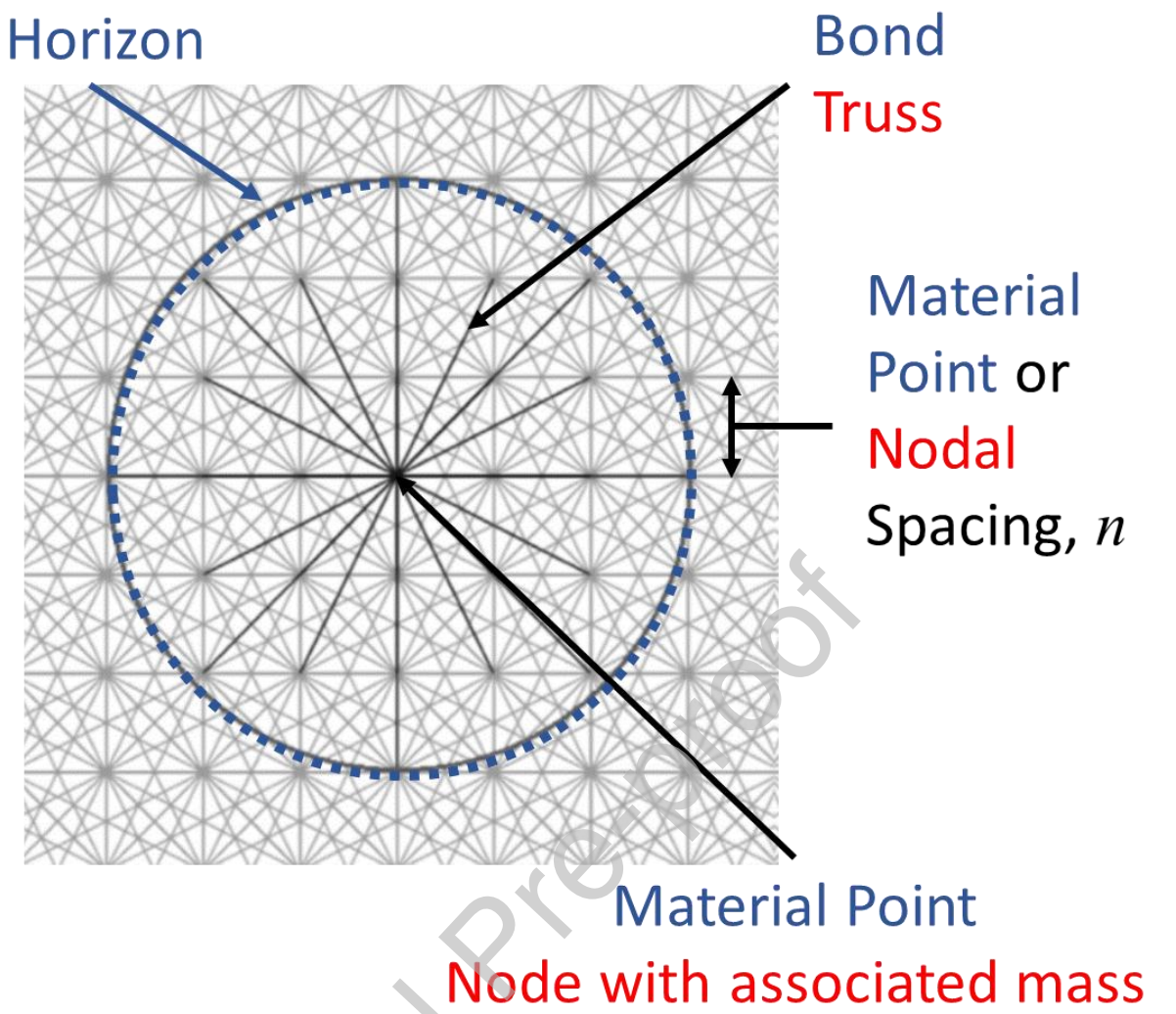

Figure 2 – An overview of the peridynamic approach taken by the authors. Terms associated with peridynamics are shown in blue and those associated with finite element analysis in red. Reproduced from Fig. 1 in [23], by permission of Elsevier under License No. 5324760658396.

2.2 Mesh & Geometric Boundary Conditions

The 2D model of a PWR fuel pellet that was developed is shown in Figure 3. The model consists of a 360° circular section through the pellet waist (mid-height elevation), which has a diameter of 8.2 mm. A Cartesian mesh was used, with a spacing of 0.1 mm between material points and the horizon ratio (the ratio of the horizon size to the material point spacing) set to 3.0. The material point spacing is below the convergence size relative to the overall mesh. It was found that going to finer meshes did not characteristically change the crack patterns or the number of radial cracks. The horizon ratio of 3.0 is typical in peridynamics work in the literature [25, 26]. To constrain the pellet, two perpendicular lines of nodes, intersecting at the centre, were restricted to have zero displacement perpendicular to the line of nodes. This forced the pellet to

expand concentrically; not to undergo linear motion; and, to avoid spurious non-physical rotation within the pellet.

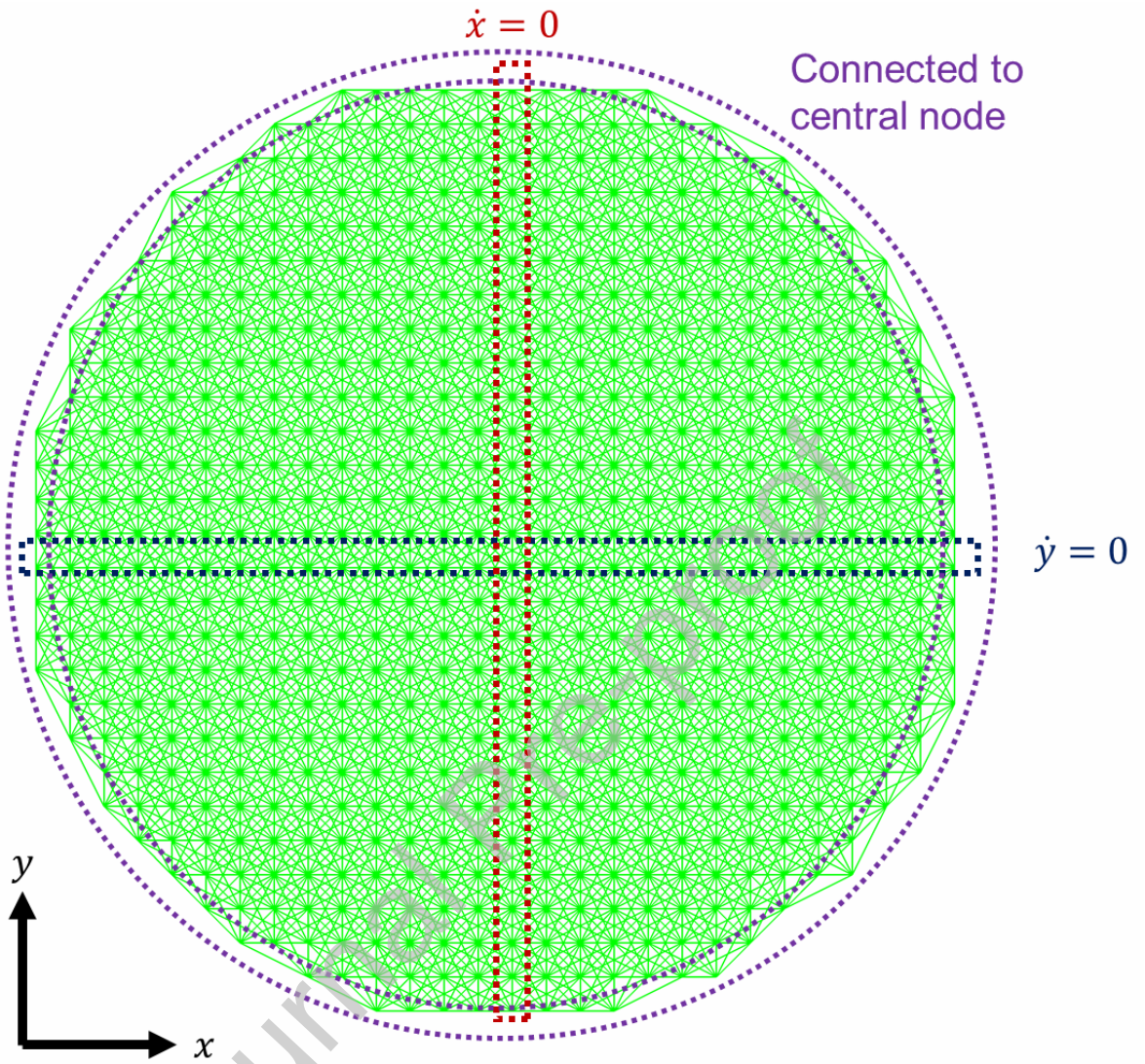

Figure 3 – A schematic of the meshing and geometric boundary conditions applied to the model.

Should the pellet fragment, these constraints are no longer sufficient, since a fragment may no longer be connected to any constrained nodes. Extra truss elements were therefore inserted, connecting the central node to all surface nodes. These truss elements have the same material properties as the main peridynamics bonds, meaning they expand at the same rate, so apply minimal force to surface nodes, causing less than a 1% variation in maximum displacement of surface nodes. They were assigned an arbitrarily high failure strain, assuring that they would never break. When a fragment breaks free from the constrained portion of the pellet, the stiffness of these additional trusses constrains the fragment.

Since the model is only of a 2D 'slice' of a pellet, the additional unbroken truss elements also act as a proxy for the remaining pellet above and below this slice, preventing the pellet from moving too freely. Without this constraint, cracks can curve artificially due to the inertia of fragments shearing away from the centre, which can lead to unrealistic crack paths growing in an outward radial direction. The effect of these additional trusses is shown in Figure 4. A possible reason for this crack curvature is the lack of including a contact behaviour between newly created crack face "surfaces" in this implementation of peridynamics. Pellet fragments are free to move without regard for contact between these surfaces, causing spurious crack curvature and branching. This movement also reduced the stability of the simulations, slowing them down, and often leading to the model crashing.

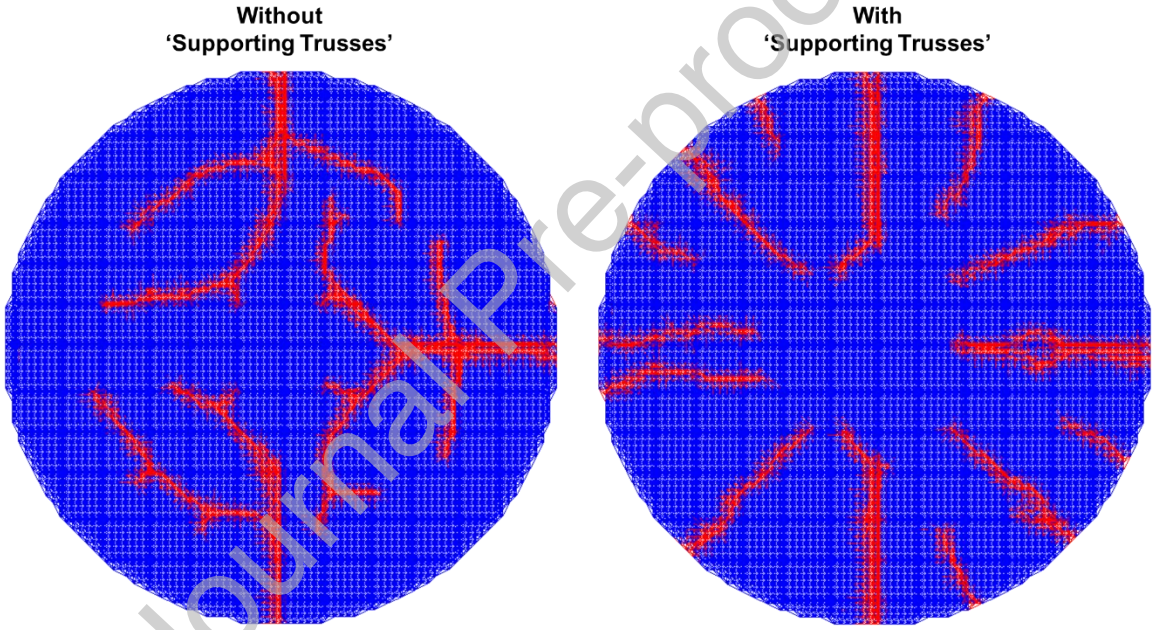

Figure 4 - Curved cracks in the absence and presence of 'supporting trusses' in pellets ramped to 40 kW m^{-1} using the bond strengths shown in Figure 6. Red shows broken bonds, blue unbroken.

2.3 Thermal Loads and Boundary Conditions

There is agreement in the literature that ramping fuel pellets to higher powers over similar periods of time results in more radial cracks around the surface of a nuclear fuel pellet, although there is some disagreement as to the provenance of such cracks. With this in mind, a test was performed to ramp pellets from a linear heat rate of 0 kW m^{-1} up to 70 kW m^{-1} over 10,000 s. The final linear heat rate of 70 kW m^{-1} is the maximum value that a PWR pellet could conceivably experience in normal operation and operational fault

conditions of a PWR. The intention was to avoid the thermal shock that has been explored in peridynamics by Oterkus & Madenci [7] and Wang et al.[13], and instead show cracking as it occurs in a fuel pellet heating up over industrial timescales of the order of days rather than seconds.

Implementing a heat transfer model in the presence of cracking can be computationally demanding and require appropriate knowledge of heat flow across the cracked surfaces. Instead, temperatures were determined by an ENIGMA fuel performance code run (NNL version, also known as ENIGMA-B [27]). The temperature data provided by ENIGMA are shown in Figure 5. The temperatures at the pellet centre and surface were applied as calculated and the remaining nodal temperatures were evaluated using a parabolic function of radius fitted to the pellet centre and surface temperature.

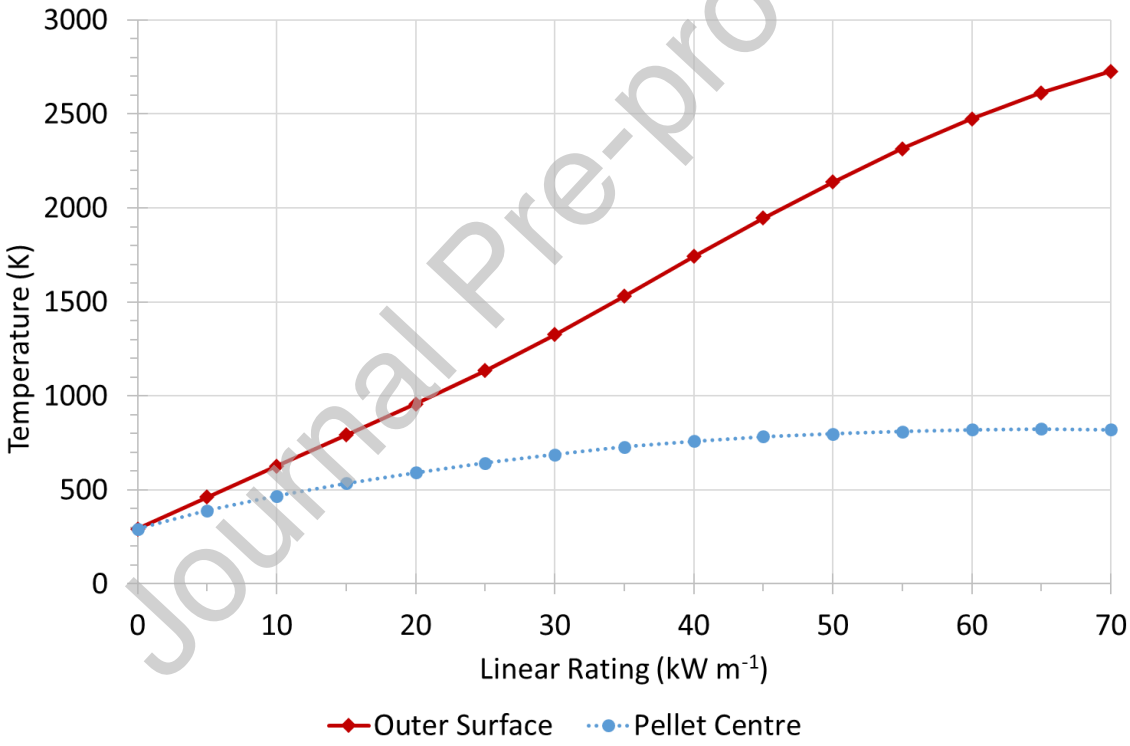

Figure 5 – The temperature data provided by the ENIGMA fuel performance code run and applied to the model and the pellet outer surface and pellet centre.

The effects of cracks on temperature distribution are not considered but given the temperature gradient is radial and cracks are radial they should have minimal impact. The modelled centreline temperature reach 2735 K at 70 kW m^{-1}. This is sufficiently close to the melting point to induce significant changes in material properties, which are for the most part neglected. The

circumferential cracks that form on the power down ramp would impact the temperature distribution at that point, but it was not believed that including this variation would affect the final radial crack numbers. Despite these limitations, this solution allows for temperature to be computed cheaply, and for a larger sample of pellet cracking simulations to be performed.

2.4 Material Properties

The UO_2 pellet was defined by the material properties given in Table 1. These values were taken from the MATPRO fuels properties library [28], assuming a pellet density equal to 95% of the theoretical value for UO_2 (i.e. assuming 5% volumetric porosity). The elastic modulus was dependent upon the absolute temperature, *T*; all other properties in the peridynamics model were not. Since pellet temperatures were prescribed in the model (see Section 2.3), values/formulae for the thermal conductivity and specific heat capacity were not required.

Table 1 - Material properties used for the UO_2 fuel simulations. Values were taken from the MATPRO fuels properties library [19]; a density of 95% of the theoretical value and temperature of 500 K were assumed. The failure strain quoted is applied uniformly and does not take into account the statistical nature of material failure.

Property	Unit	Value / Formula
Elastic Modulus	Pa	$2.013\text{x}10^{11}(1 - 1.0915\text{x}10^{-4}T)$
Failure Strain	-	$5.34\text{x}10^{-4}$
Coefficient of Thermal Expansion	K^{-1}	$1.0\text{x}10^{-5}$
Theoretical Density	kg m^{-3}	$1.096\text{x}10^{4}$

The failure strain of bulk material was set to $5.34\text{x}10^{-4}$, representative of a stress of 100 MPa at 500 K and in-line with the range of 50-160 MPa typically discussed [12, 29, 30]. This value was also used as the characteristic value in the Weibull distribution for the failure strain of near-surface material. The variation in failure strain with temperature was considered outside the scope of the work.

2.5 Implementation of Weibull Statistics

Previous work, [19], has shown that it is possible to recreate Weibull distributions with reasonable accuracy in a two-dimensional representation of a tensile test. The surface of an expanding circle, such as the pellet slice

modelled in this work, may be considered analogous to the surface of a two-dimensional tensile test specimen, since the surface stress is ostensibly uniformly distributed in both cases. Two-dimensional Weibull peridynamic bodies have an additional complication relative to one-dimensional peridynamic bodies in that crack propagation must be considered. This is doubly true in the fuel pellet scenario, as the hoop stress at the tip of ingrowing radial cracks decreases as the cracks grow inward, and the tip moves towards the centre of the pellet, where the stress is compressive.

In contrast to real materials, initiation and propagation of cracks in two-dimension peridynamics bodies of the kind modelled in this work are fundamentally separate processes. In real brittle materials, Griffith's criterion [31] describes the process of crack growth, and allows only for growing, shrinking and (in equilibrium) stable cracks. It makes no mention of the initiation of cracks. Cracks are presumed to exist, in a way that they do not in continuum models. This difference is the reason for the randomisation of the properties of some bonds in order to recreate the properties of a Weibull distribution.

Conversely, Weibull makes the opposite assumption about fracture. There are no rules for the growth of cracks, only initiation. Fracture in Weibull analysis is a single event, not a process. This contradiction can be reconciled by having Weibull behaviour govern the failure of bonds involved in fracture initiation (i.e. surface bonds), with the failure of bonds in bulk material governed by a single value strain criterion. Inherent to this method is an assumption that cracks initiate solely on the surface which, given the stress profile, seems a safe one. Through this split-regime method, crack initiation can be defined by strain as this was shown by the authors to be possible to calibrate to a Weibull distribution in [19]. Given the potentially large differences between the bulk values and the Weibull-randomised surface values, it was necessary to create a near-surface region of thickness equal to one horizon radius (i.e. three nodal spacings) for the Weibull values; this is shown in Figure 6. This allows for nucleated cracks to grow a small distance while still governed by the Weibull values. Once cracks reach bulk material, the initiation of cracks due to Weibull behaviour is no longer appropriate and a uniform fracture strength was applied. Using a fracture mechanics-based criterion (i.e. a critical energy

release rate) would perhaps have been more appropriate for this region, but would have considerably increased the complexity of the work.

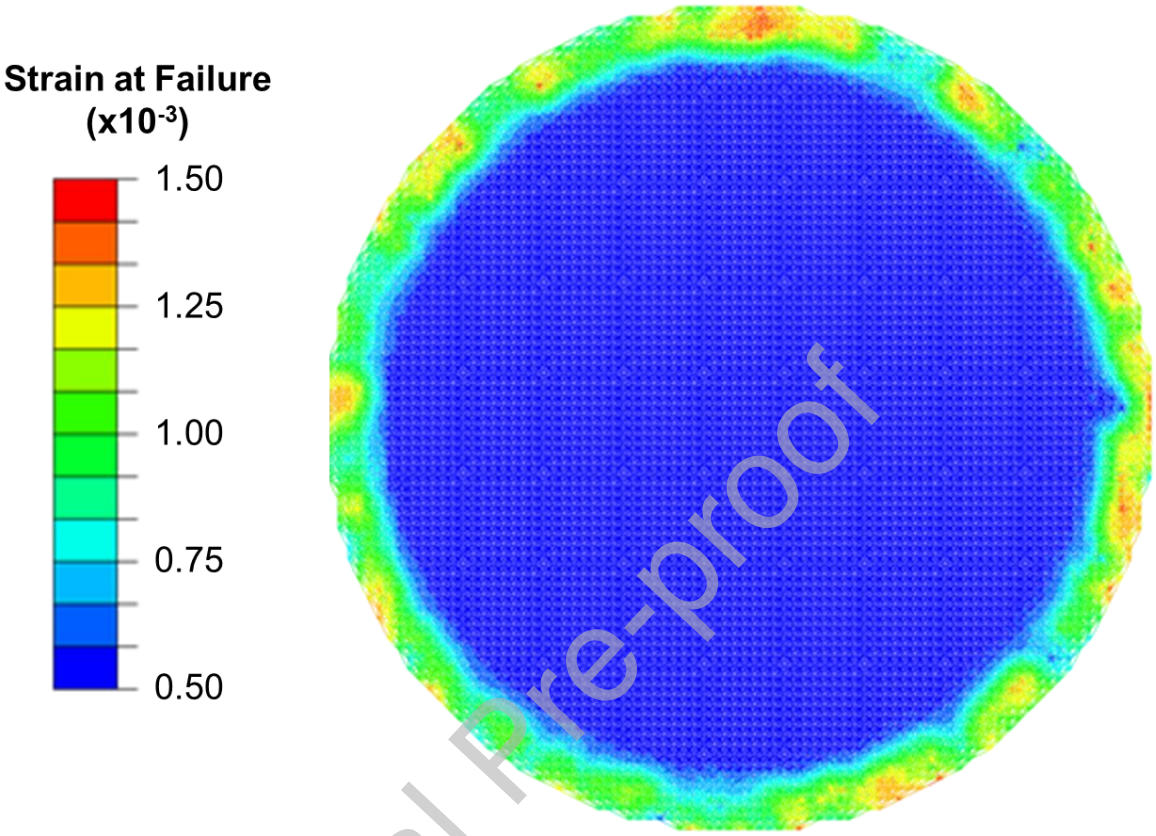

Figure 6 - The failure strains of bonds attached to nodes within one horizon of the surface were randomised according to a Weibull distribution, with Weibull modulus β = 10, characteristic strain ε_0 = 5.34x10^{-4} and using size scaling to account for the difference in size between peridynamics bonds and the pellet. The failure strains of bonds in the bulk were assigned a fixed value equal to the characteristic strain.

Size scaling of the surface was carried out by determining the total number of material points within the horizon-radius-thick near-surface region, *N*, and using equation (2), in which ε_{Sc} is the scaled fracture strain, ε_0 is the failure strain of the sample and β the elastic modulus. This is the same approach as taken by Strack et al. [20] for the volume of the simulated specimen.

$$\varepsilon_{Sc} = N^{1/\beta}\varepsilon_0 \qquad (2)$$

Whilst ceramics of this type would usually conform to a volume-scaling throughout, the nuclear fuel pellet is a special case due to the parabolic temperature profile creating a very strong tensile stress on the outer surface.

The distribution of flaws on the outer surface are therefore of much greater importance than those in the bulk of the pellet, justifying a surface-scaling approach. This is further justified by our successful validation against PIE. Unlike other models [6, 12, 32], we have applied a uniform fracture strength to the bulk of the pellet. Once cracks start growing, they were observed to continue; the agreement between the model and PIE is discussed withing the text. Furthermore, it should also be noted that the pellets are contained within a metallic cladding. Once the pellet has cracked, the fragments will move radially outwards in a process termed 'relocation' [1, 10, 33]. Once contact is made between the pellet fragments and cladding (termed soft-PCI), the motion of the fragments and therefore the dissipation of energy will be affected by the cladding. The application of a uniform fracture strain within the component volume is less appropriate to materials such as reactor pressure vessel steels which contain regions that are not truly brittle. These ductile regions can lead to crack arrest and pop-in behaviours [34].

2.6 Computational Experiments

Since the work is of an inherently statistical nature, some thought is required to determine an appropriate sample size. Typically, a larger sample size will produce results more representative of the population, but that would not necessarily be a fair like for like comparison to the PIE data in this case. Using a larger sample size would lead to an increased likelihood of predicting a low probability event, such as a very large number of cracks, which would skew the predicted distribution of the number of radial cracks in a non-physical way. This could lead to an increase in the N_∞ parameter, simply as a result of observing a larger sample size. In reference [10] a total of 45 pellets, after ramping to a range of powers from 7–65 kW m^{-1}, were observed. This is replicated in the peridynamics simulations, with 45 pellets modelled, each ramped to a power corresponding to one of the pellets observed in [10]. Each of the 45 models used a different random seed to obtain the Weibull failure signs assigned to the material points.

In order to measure the closeness of fit between the data from [10] and that from the peridynamics simulations, the formula (given in (1)) used by Barani et al. [11] to fit a curve to the data from [10] was used to plot a line of best fit for the peridynamics data. The parameters were restricted to the integer values

which produced the lowest χ^2 compared to the simulation results. The difference between the parameters used by Barani et al. and those used for the peridynamics models serves as a measure for the difference between the Walton and Husser data and the peridynamics predictions.

Despite the lack of pellets ramped to less than 5 kW m^{-1}, this linear heat rate is a reasonable estimate for the power at first cracking, $\dot{q}'_0$, and so was kept fixed to the Barani et al. value [11] for all fits. The same is true for the number of cracks at first failure, N_0.

Finally, to briefly demonstrate the necessity of some level of failure strain randomisation, a pellet was simulated with near-surface bond failure strains randomised according to a distribution with arbitrarily large Weibull modulus of 10^5, i.e. with a good approximation to a single failure strain applied uniformly.

3 Results & Discussion

3.1 Infinite Weibull Modulus

Differences in failure strain for the pellet with Weibull modulus of 10^5 were negligible and this is reflected in the results in Figure 7(a).

The pellet fractured symmetrically, with eight radial cracks initiating on the points most distant from the centre at around 5 kW m^{-1}. It continued to fracture symmetrically, with multiple cracks initiating at once, in three separate fracture events, reaching twenty radial cracks at 44 kW m^{-1}, with no increase in the number of cracks at higher linear heat rates. Twenty distinct cracks, as shown in Figure 7(b), is more than would be expected based on the Walton and Husser data, and they occur in a pattern that does not fit the PIE data or the curve from Barani et al. [11].

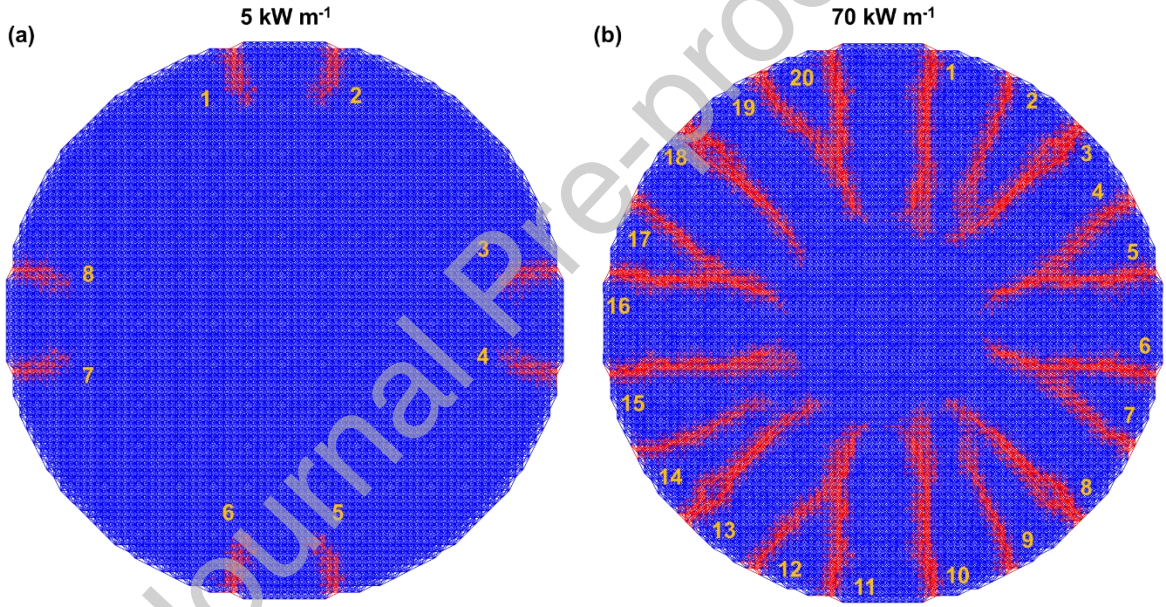

Figure 7 - The extent of cracking in the $\beta = 10^5$ case at (a), 5 and (b), 70 kW m^{-1} Red shows broken bonds, blue unbroken.

One facet which is possible to ascertain in Figure 7(a) is the impact of implementing the constraint along the *x* and *y* axes, described by Figure 3. This, together with the rectangular mesh has the effect of effectively splitting the pellet into four approximately symmetric domains. It should be noted that that due to the non-locality of peridynamics and overlapping bonds across the constraints, there will be some form of stress transmission from region to region. The symmetry effects seen in Figure 7(b) are therefore less

pronounced. Since this is a high-power scenario, the cracks can be seen to be fairly uniform and therefore not dominated by the initial boundary conditions.

When the relationship of number of cracks against the linear heat rate at which they occur is plotted, as shown in Figure 8, it does not seem to show the characteristic exponential shape as described by Barani et al. [11]. The best possible fit of a Barani-type exponential curve was to use parameters of $N_0 = 8$, $N_\infty = 20$, $\dot{q}'_0 = 5$ kW m^{-1}, and $\tau = 5$, although with only three data points, the curve does not fit the data well, and the parameters were calculated only for the purposes of comparison to later curves. Repeated simulation using such a high Weibull modulus yielded the same result, as expected. For that reason, the peridynamics data in Figure 8 represent only one simulation. Each time new cracks nucleated in the simulation, the power and number of cracks were recorded, and this data is presented in Figure 8. This differs from the way crack numbers were recorded for the other cases.

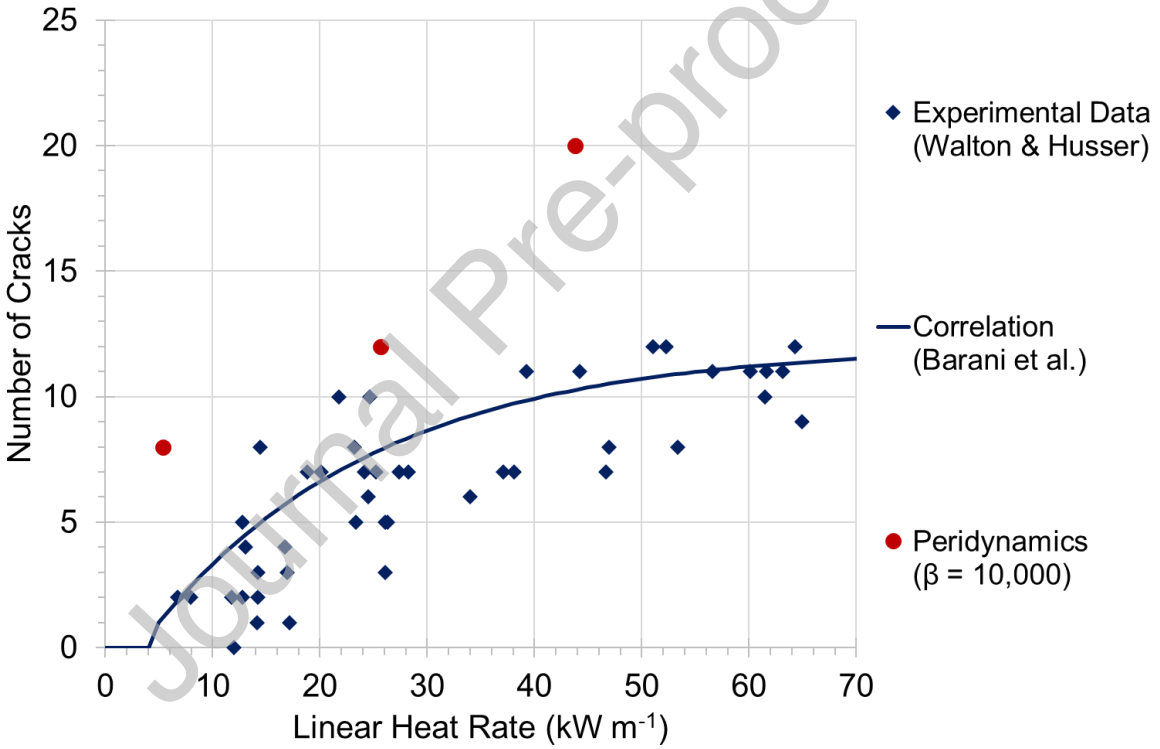

Figure 8 – Predictions and measurements [10] of the number of radial cracks versus linear heat rate. Predictions are with a Weibull modulus $\beta = 10^5$ but with no size scaling to account for the difference in size between bonds and the overall object compared to the curve Barani et al. [11] plotted to fit the PIE data in [10]. It should be noted that due to the effectively infinite modulus, the three data points shown for the peridynamics simulations are in effect three snapshots of essentially the same simulation.

3.2 Realistic Weibull Modulus

To overcome the poor predictive performance of the simulations shown in Figure 8, a randomisation scheme using a Weibull shape modulus of 10, but with no size scaling was employed. This corresponds closely to the Gaussian randomisation used in reference [7] and is not too dissimilar from the Weibull distribution used by Li and Shirvan [8]. As shown in Figure 9, plotting a Barani-type curve [see equation (1)] using the best-fit parameters of $N_0 = 1$, $N_\infty = 25$, $\dot{q}'_0 = 5$ kW m^{-1}, and $\tau = 30$ against the curve fit to the Walton and Husser data shows a considerable overestimation in the number of cracks predicted at a given power, in relative terms at low power, and in absolute terms at higher power.

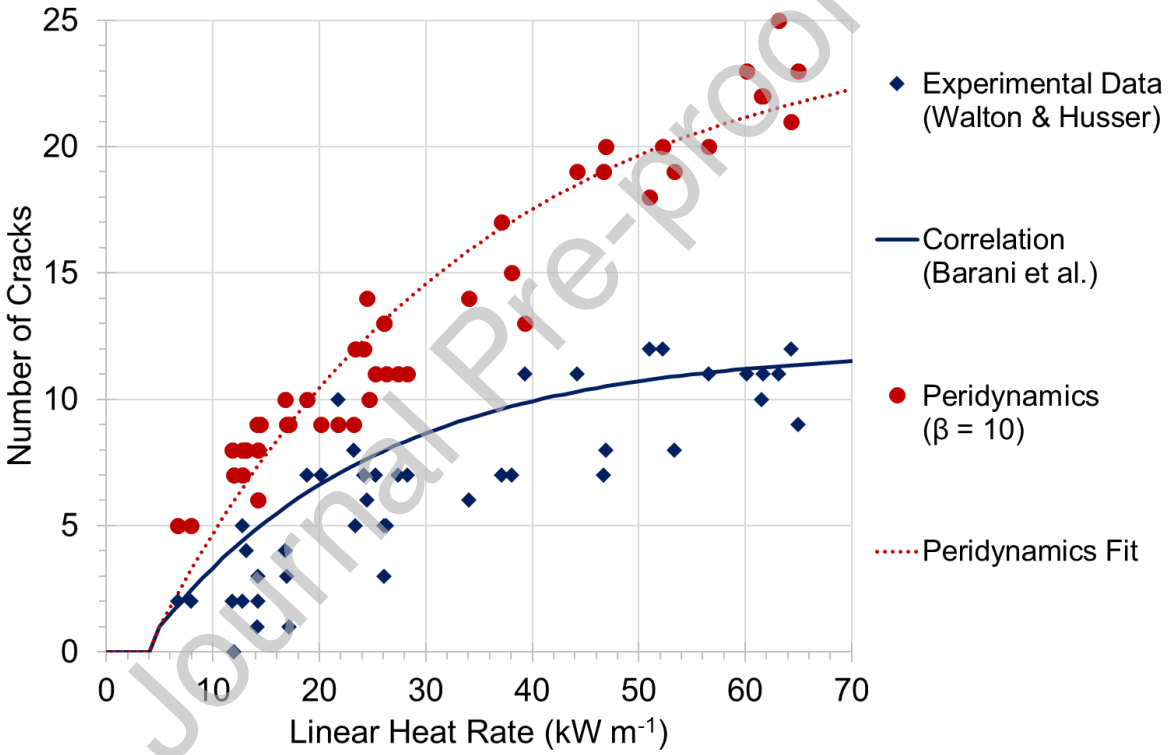

Figure 9 - Predictions and measurements [10] of the number of radial cracks versus linear heat rate. Predictions are with a Weibull modulus $\beta = 10$ but with no size scaling to account for the difference in size between bonds and the overall object compared to the curve Barani et al. [11] plotted to fit the PIE data in [10].

3.3 Sample Size Scaling

By using the size-scaling method outlined in Section 2.5 and keeping the Weibull modulus at 10, the difference between the simulation predictions and PIE data can be reduced. Fitting an exponential curve to the predictions produces the parameters $N_0 = 1$, $N_\infty = 17$, $\dot{q}'_0 =$ 5 kW m^{-1}, and $\tau = 25$. As shown in Figure 10, the predictions fit better to the curve for the experimental data from [10] up to around 30 kW m^{-1}, but with increasing power the difference becomes significant, with the measured number of cracks overpredicted.

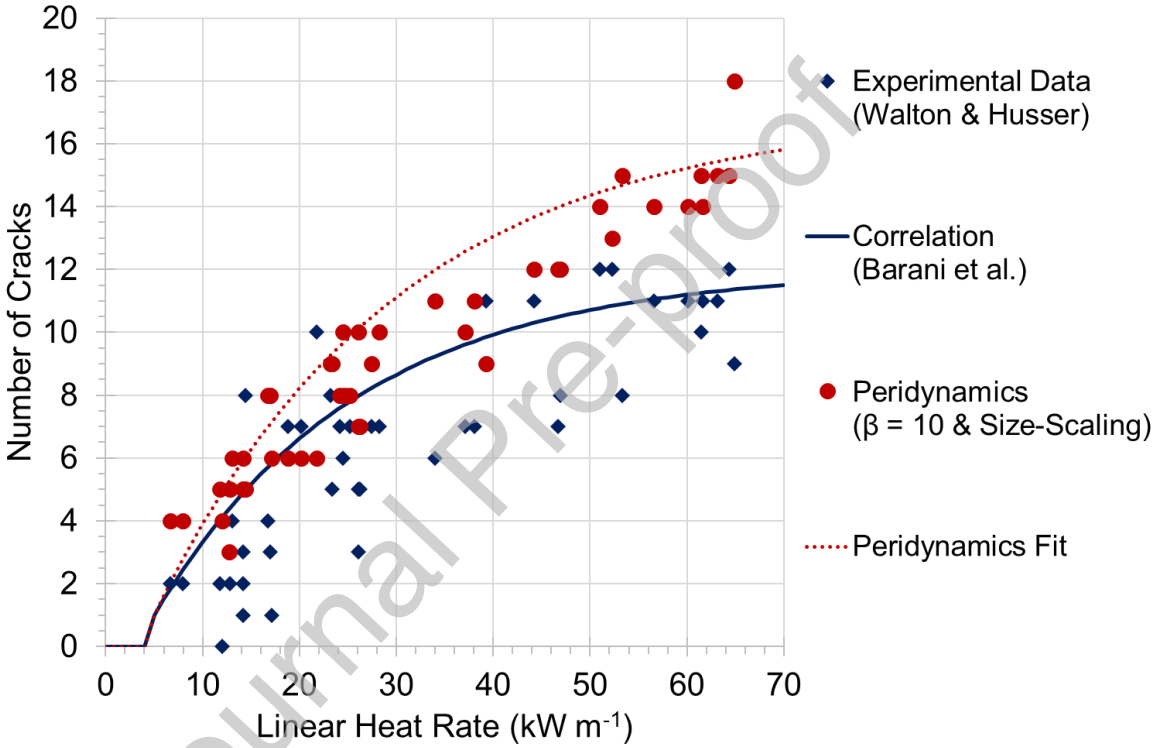

Figure 10 - Predictions and measurements [10] of the number of radial cracks versus linear heat rate. Predictions are with a Weibull modulus $\beta = 10$, together with size scaling to account for the difference in size between bonds and the overall pellet. Comparison is made to the curve Barani et al. [11] fit to the PIE data in [10].

Since the peridynamics simulations still result in significantly more cracks than were observed in the PIE data, and there is evidence that using broader Weibull distributions (i.e. $\beta < 10$) produces lower crack numbers at very high power, which would be a better fit to the data in [10], the experiment was repeated with a Weibull modulus of 5. In Figure 11, there are several predictions of 13 cracks at high powers, which is greater than the maximum number of cracks than observed by Walton and Husser N_∞ of 12 set, based on the Walton and Husser data, but otherwise the predictions are a good fit to the curve that best describes the Walton and Husser data. The parameters used to fit to the peridynamics model predictions were $N_0 = 1$, $N_\infty = 13$, $\dot{q}'_0 = 5$ kW m^{-1}, and $\tau = 25$.

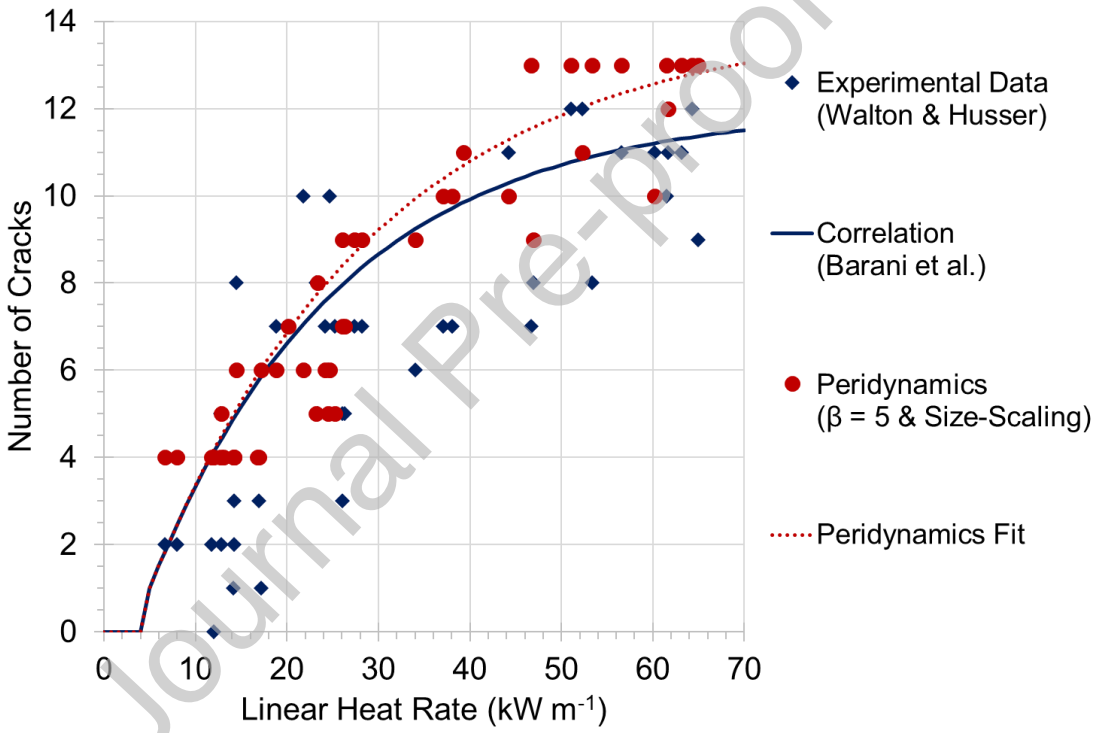

Figure 11 - Predictions and measurements [10] of the number of radial cracks versus linear heat rate. Predictions are with a Weibull modulus $\beta = 5$, together with size scaling to account for the difference in size between bonds and the overall pellet. Comparison is made to the curve Barani et al. [11] plotted to fit the data in [10].

3.4 Simulation Artefacts

A Weibull modulus of β = 5 is not fully supported by the method set out in [19], as it is below the lower bound of β = 7.5 determined in [19]. Using a Weibull modulus this low introduced a possibility for cracks to initiate in the bulk region, away from the surface, as shown in Figure 12. Using this method, there is a possibility for cracks to initiate in the near-surface region. This is not a good representation of the behaviour of the material since all cracks observed in PIE are seen to originate at [or perhaps extend to] the outer surface. These cracks were counted as surface cracks for the purposes of Figure 11.

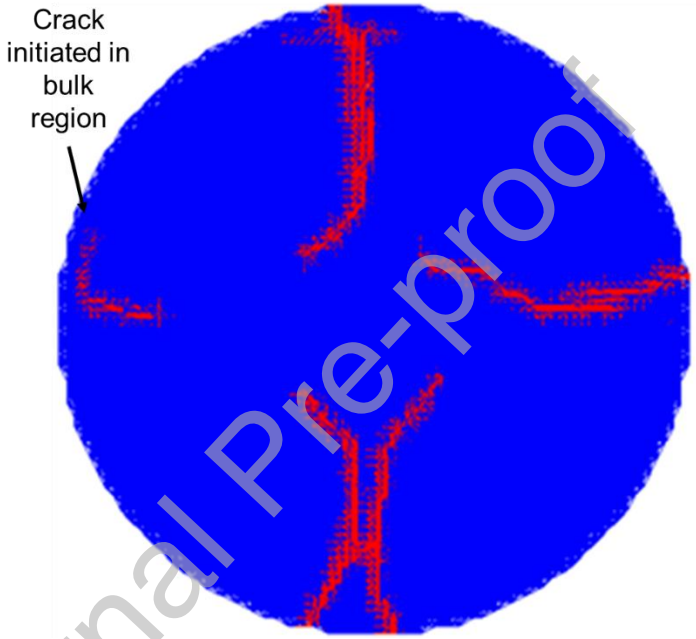

Figure 12 - A pellet simulated with a Weibull modulus β = 5, with an arrow highlighting a crack which nucleated in the bulk region of bonds, rather than at the surface. Red signifies broken bonds.

In Figure 12, the effect of implementing the constraint along the *x* and *y* axes (shown in Figure 7 and described by Figure 3), can be seen to have been removed. The pellet no longer appears to be split into the pellet into four symmetric domains. There appears however to be a secondary phenomenon whereby cracks 'reflect from' the symmetry applied along the *x* and *y* axes. Future work could focus upon either reducing the extent of symmetry or exploiting it to run the simulations more quickly.

3.5 Summary of Fitting Parameters

The parameters used to plot the curves in Sections 3.1 to 3.3 are collated in Table 2. Case 1 is the so-called naïve approach with essentially zero randomisation of material fracture strengths. Case 2 is the approach designed to be reasonably close to that of the fracture distributions used in other works, without surface size scaling. Case 3 uses the same Weibull modulus, (i.e. one that is reasonable for a ceramic of this type) but also includes the size scaling effect between bonds in the peridynamics model. Case 4 is the attempt to attain a closer fit to the PIE data in [10] by means of using a smaller Weibull modulus. Although Case 4 shows the best fit to the experimental data, the artificial crack nucleation it shows means care must be used with such low Weibull moduli. Case 3 is therefore most appropriate for guiding future work, especially for powers below 30 kW m^{-1}, at which LWRs typically operate. Care would be needed when simulating high power accident conditions using this method.

Table 2 - Parameters used for fitting curves in Sections 3.1 to 3.3

Case	Weibull Modulus β	Size - Scaling	Characteristic Failure Strain	Fitting Parameter τ	Maximum Number of Cracks N_∞
1	10^5	No	5.34×10^{-4}	5	20
2	10	No	5.34×10^{-4}	30	25
3	10	Yes	5.34×10^{-4}	25	17
4	5	Yes	5.34×10^{-4}	25	13
Experimental Data	-	-	-	*21*	*12*

3.6 Behaviour during Power Decrease

Figure 13 shows the crack profile of a pellet ramped over 10,000 s to a linear heat rate of 70 kW m^{-1} before holding for 10,000 s and then ramping down over 10,000 s to 0 kW m^{-1}. Notable features include:

- Nucleation of a single crack at ~5 kW m^{-1} as predicted by Walton and Husser [10].
- Some evidence of hierarchical crack growth, with alternating longer and shorter cracks, particularly in the higher power images.
- No additional radial cracks nucleate on the entirety of the ramp down, although in a few cases circumferential crack growth originating at the tips of radial cracks can be seen at the end of the ramp down.
- Radial cracks initiating at the tips of other approximately radial cracks, for example at 45 kW m^{-1}. Although this growth could be an expression of a real physical phenomenon, it is more likely an artefact resulting from stress in the support trusses.

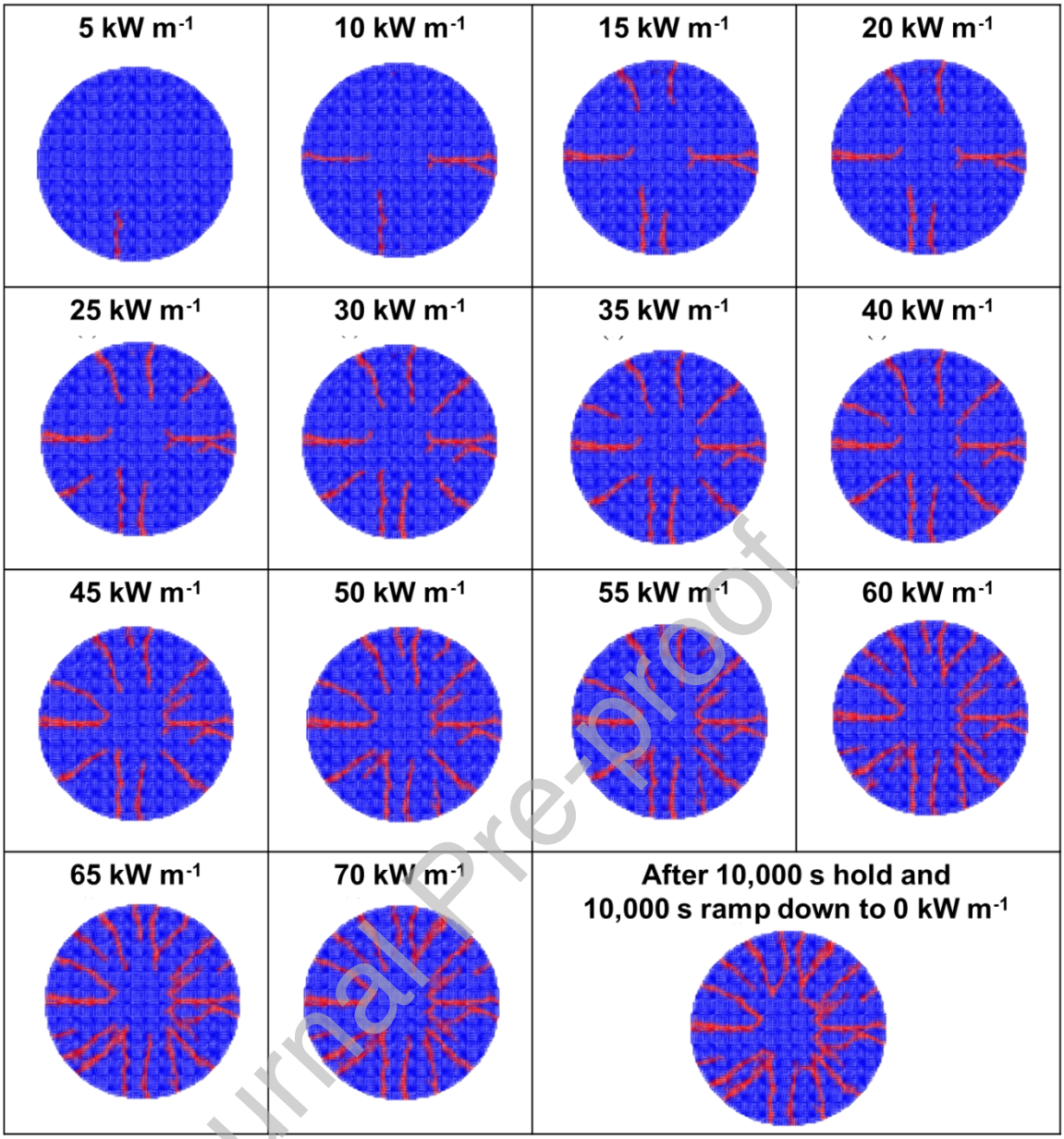

Figure 13 - Crack patterns predicted by a peridynamics model of a UO_2 pellet ramped to 70 kW m^{-1} over 10,000 s; held at power for 10,000 s; and then ramped down to 0 kW m^{-1} over 10,000 s. Red shows broken bonds, blue unbroken.

The method of using support trusses to prevent overlapping of the pellet fragments causes the pellets to display similar crack patterns regardless of Weibull modulus, with the exception of the symmetry in Case 1 of Figure 14. The cracks are broadly straight, radial in nature and originate at the surface. In most cases there is also evidence of hierarchical crack growth, where the growth of roughly every second crack is stunted by the neighbouring cracks. It is, however, worth commenting on what effect a variation in radial crack number might have in reality. In [35], deviations in direction can be seen in

what might be expected to be straight cracks where cracks are more isolated. This can be seen to some degree in some of the pellet modelling in the literature, particularly that of Huang et al. [6]. Cracks that deviate from a purely radial direction, i.e. do not grow directly towards the centre of the pellet, could affect the radial heat flow of the pellet, but the degree to which this is the case is not clear and not measurable by experiment. In any case, circumferential cracks are likely to grow on the first cool down of the pellet's lifetime, so the effect of radial crack curvature would be obscured by this.

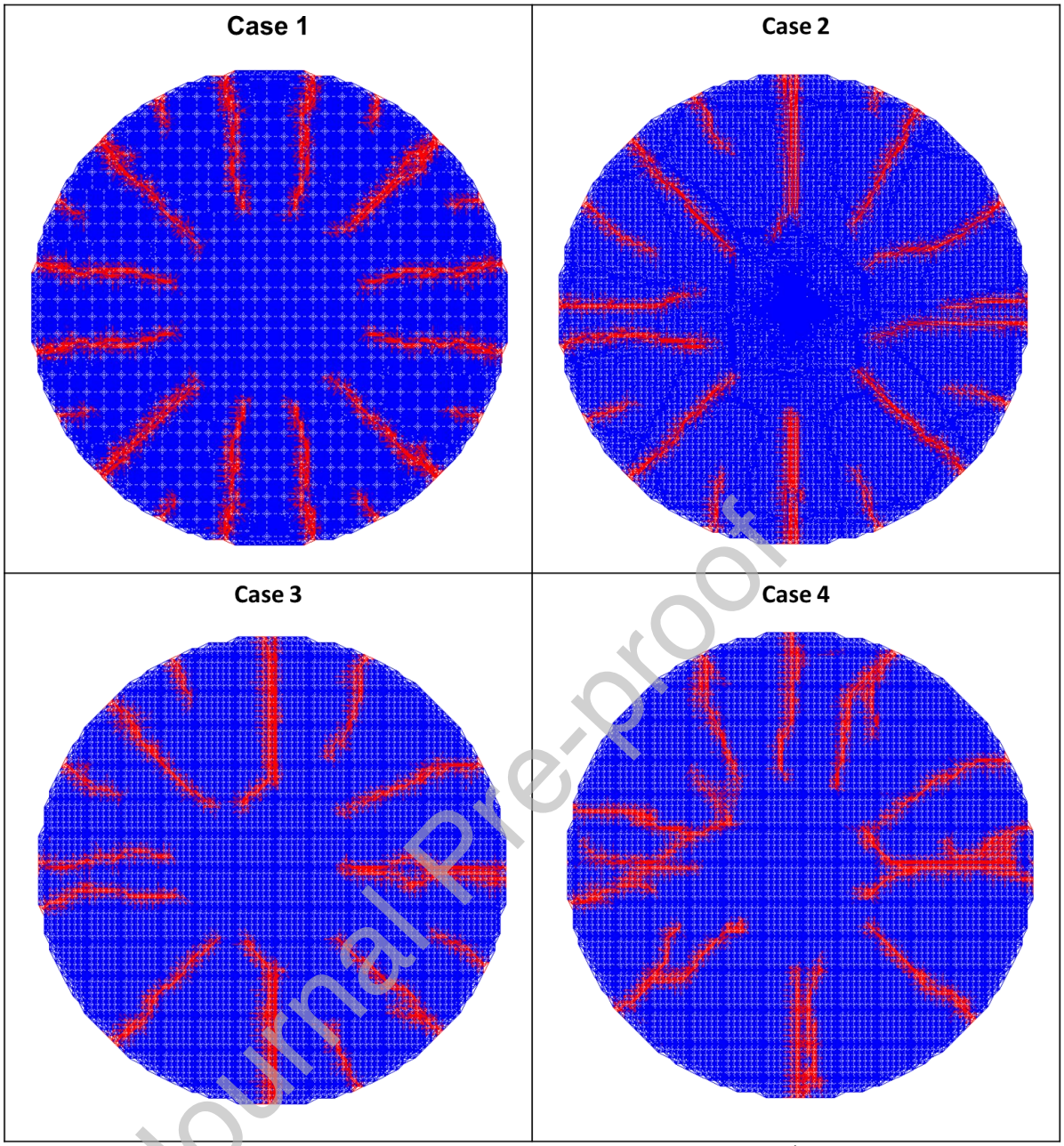

Figure 14 - Crack patterns after ramping up to 45 kW m^{-1} over ~6,500 s using Cases 1-4 bond strength randomisation. Red shows broken bonds, blue unbroken.

Also visible in Figure 14 is a tendency for some, but not all, cracks to initiate on geometric features of the mesh. This is in part a feature of modelling a curved surface using a rectangular mesh and is in-part offset by the use of the edge correction term detailed in [23].

3.7 The Use of Randomness in Modelling Nuclear Fuel Pellets

The Walton and Husser data suggests that the number of cracks that nucleate with respect to power decreases with increasing power, since the number of

cracks is an inverse exponential function of the linear heat rate. The explanation for this, which fits with the data in this work, relates to the interaction between stress and crack numbers. If there are more cracks, more strain energy is expended on the growth of those cracks as power increases. This increases the amount of power required to produce the same stress at the surface. If there are more cracks, the surface length between them is smaller, reducing the stress. The first crack appears at the weakest point on the surface of the pellet, and each subsequent crack will appear at a point on the surface that is stronger. If strength were the only determining factor, this effect would not be noticeable in a real pellet, with a vast number of possible crack initiation sites. However, crack initiation tends to occur in exactly the middle of two other cracks, where the stress is highest, falling off to zero with decreasing distance from the nearest crack. This whole process means each crack samples a smaller line segment in the 2D model (surface area in 3D) than the preceding cracks, which will effectively increase the characteristic strength of the material for each new crack.

Using nominal randomisation of strengths on the order of Weibull modulus β = 10 with no size scaling has some benefit, in that the symmetrical effects of the mesh are lessened. There is still an element of symmetry to the final crack patterns, owing to the square, relatively coarse nature of the mesh used. Perhaps the most notable advantage of this degree of randomisation is to allow individual cracks to occur, rather than nucleating many at once. This means the number of cracks in the pellet follows a smoother trend with respect to the increase in power. This is the only significant difference between this randomisation scheme and the no randomisation scheme. This makes sense, since the express goal of this nominal randomisation in other work is to avoid the qualitative problems associated with a homogeneous strength distribution, without changing the quantitative results.

Introducing near-surface size scaling produces a much greater degree of randomisation (the amount that would realistically be seen in a ceramic like a UO_2 fuel pellet). This better reproduces the observed linear heat rate increments between each crack nucleation event whilst reducing the maximum number of cracks to be more in line with the Walton and Husser PIE data. Reducing the Weibull modulus further produces an even better fit to this data,

but in the cases shown here produces artificial crack nucleation behaviour. This issue stems from the fact that bond failure is determined by failure strains, assigned with the goal of reproducing Weibull distributions, which govern crack initiation, but make no prediction about crack growth. The interior bonds fail at strain greater than 5.34×10^{-4}, the characteristic strain of the Weibull distribution, based on the literature value for UO_2 fracture stress [28]. Due to the Weibull distribution scaling, surface bonds typically fail at much higher strains, with only isolated instances of lower failure strains, dictating where cracks nucleate. In the low Weibull modulus ($\beta = 5$) case, this is more pronounced, producing cracking in the interior, which is now, in places, weaker than the surface. Bonds on the surface being stronger than those in the interior is at odds with the reality that the surface contains bigger flaws, and is therefore 'weaker' in reality. This bond strength scheme is used only to achieve the required Weibull-type behaviour. Using a different failure criterion for the interior bonds could be justified, since the strain criterion is intended to control the initiation of fracture, rather than the growth of cracks. What is clear is that the reduction in the number of cracks nucleating in a given linear heat rate increment with increasing linear heat rate is more accurately described when applying a reasonably accurate amount of material strength randomisation. The exact optimal value of Weibull modulus, β is not fully defined by this work, but it is clear that a value in the region of 5 – 10 would be sensible.

3.8 Comparison of Models and Post-Irradiation Examination Data

The current model has no capacity to model frictional contact between crack surfaces and so ramping down power does not necessarily produce representative results. Assessing the crack patterns against PIE data must therefore be approached with some caution. Comparing to other explicit cracking methods, as done in Figure 15, shows a good similarity with some, with cracks growing toward the centre but not penetrating into the central compressive stress zone. This may not be an entirely accurate description of the behaviour of real crack growth. It does not fit the pattern described by Oguma [1] nor does it particularly closely match the schematics outlined by Walton & Husser [10]. This uncertainty around the behaviour in the bulk of the pellet is more reason to avoid fitting too exactly to the Walton and Husser data, since this behaviour affects the number of cracks nucleating with increasing power. A more robust model of crack growth in the bulk of the

pellet would be required before fine tuning the initiation behaviour any further.

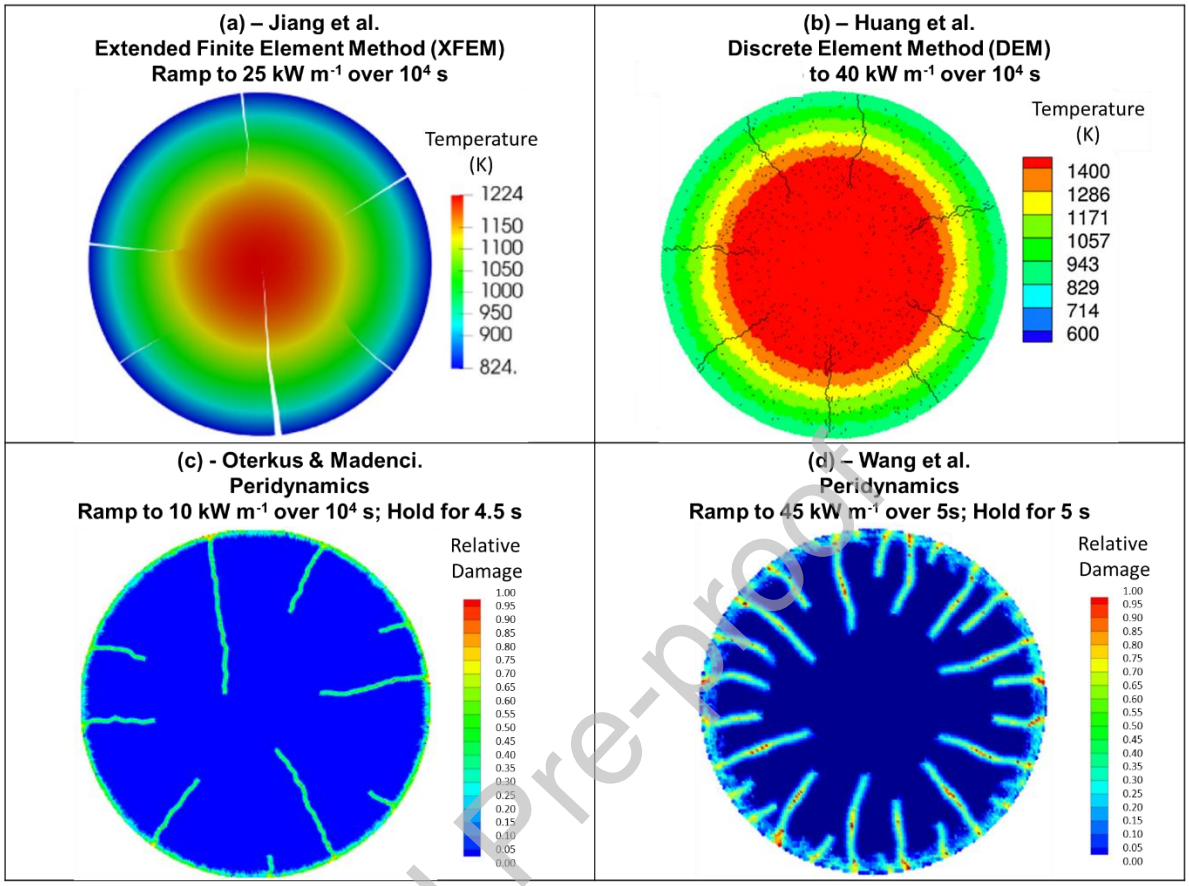

Figure 15 – Fracture patterns predicted using: (a) XFEM by Jiang et al.; (b) DEM by Huang et al., (c) peridynamics by Oterkus & Madenci; and, (d) peridynamics by Wang et al. Reproduced from: Fig. 19 in [12], Fig. 11 in [6], Fig. 11. in [7] and Fig. 13 in [13] by permission of Elsevier under License Nos. 5324761120197, 5324761237173, 5324761457778 and 5324770080623.

The simulations by Wang et al. [13] predicted that circumferential cracks nucleated on crack surfaces upon ramping down the linear heat rate. This crack pattern, shown in Figure 16, is presented by Wang et al. in comparison to the PIE crack patterns, also shown in Figure 16, as evidence of accuracy in representing PIE crack patterns. From this, the conclusion can reasonably be drawn that the peridynamics simulations run for this work are a reasonable representation of the behaviour of real pellets, given that they are a good match to the simulations carried out by Wang et al. and that they are in turn a good match to PIE image published by Michel et al. [36]. It should however be noted that PIE images cannot tell you *when* circumferential cracks in fuel pellets are formed. That no additional radial cracks initiate on the surface on

the power down-ramp is evidence that the crack numbers recorded in this work can be compared with the Walton and Husser data, as done here.

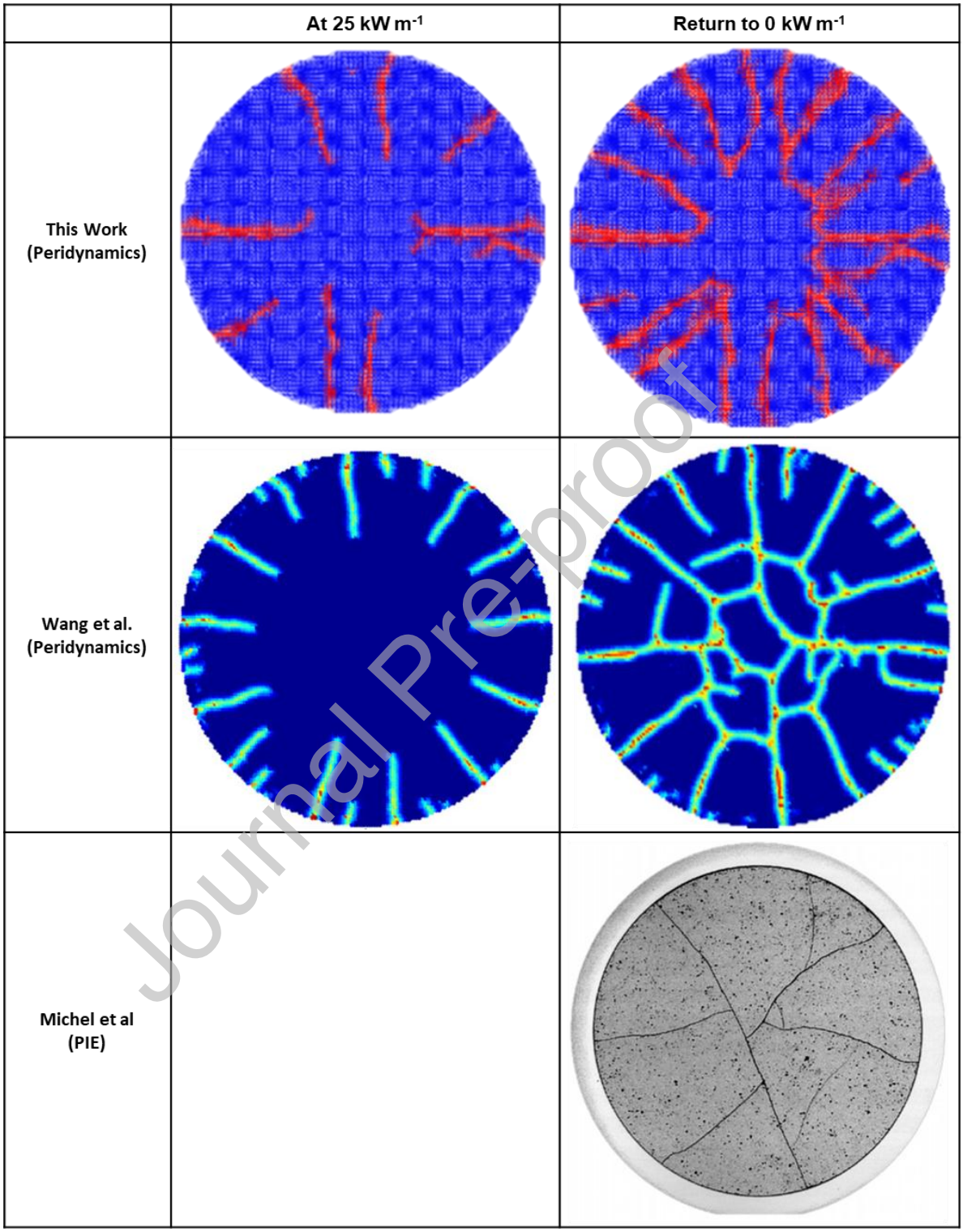

Figure 16 – Fracture patterns predicted by this work; predicted by Wang et al. (reproduced from Fig. 18 in [13] by permission of Elsevier under License No 5324770239228); and, observed in PIE and reported by Michel et al. (reproduced from Fig. 4 in. [36] by permission of Elsevier under License No 5324770402722).

A notable difference between the modelled crack patterns and PIE images is an absence of cracks from surface to surface through the central region of the pellet, of the kind outlined by Oguma [1]. Given that Oguma's is a relatively simple analytical model compared to modern numerical models, there should be no rush to alter models to match its results. Cracks of this type do seem to appear in PIE though; a candidate for such cracks are shown in Figure 17. The reason for the absence of such cracks in the explicit numerical methods explored here is not clear. It may be caused by over-constraining the mesh in the central region.

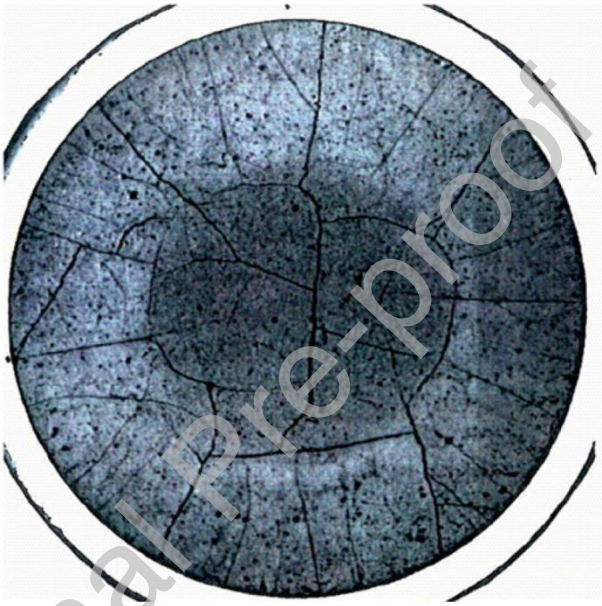

Figure 17 – Crack patterns observed in PIE after a power ramp test to 40 kWm^{-1}. Reproduced from Fig. 18 in. [36] by permission of Elsevier under License No 5324770402722.

Due to the computational demand of the techniques presented in this paper, together with those shown in Figure 15, the models all ignore cracking in the *r-z* and focus only on the *r-Θ* plane. Cracking in the *r-z* plane is likely to relieve stress in the *r-Θ* plane and impact the predicted crack patterns in the *r-Θ* plane. Future work in 3D will hopefully determine the impact of this. Nevertheless, by validating the current model against data from PIE, the appropriateness of the 2D (*r-Θ*) assumption can be partially ensured.

To date, Mella and Wenman's paper [14] is one of the few in 3D. It should be noted however, that this was carried out for annular pellets currently employed in the UK's AGR fleet.

Work on further validation of models such as the one detailed in this paper is ongoing. On the modelling side, recent work by Gamble has used a volume-scaled Weibull distribution [37] in a model built based on XFEM. Their work is currently limited to radial cracks, whilst our work using peridynamics is able to model a wide range of crack morphologies including branching. The need to model complex crack morphologies has been highlighted by Spencer et al.'s [38] recent experimental data. On the experimental side, Patnaik et al. [39] performed experimental work heating UO_2 pellets resistively and observed cracking when the difference between the surface and centreline temperatures was around 200 K. In the peridynamics simulations in this work, the temperature difference at first cracking was around half this value. This may be explained by the fact that the pellet surface temperature was much higher in the experimental work than would be expected in-reactor, at 1500 - 1600 C. The methodology used (resistive heating) meant that generating larger temperature differentials was impossible, and thus only one cracking event was observed. Most recently,

4 Conclusions

- The model presented is based on a 2-dimensional application of Weibull theory to peridynamics, that can recreate the observed relationship between pellet radial crack number and linear heat rate, in low-burnup nuclear fuel, with reasonable accuracy, relative to available PIE data.
- The measured dependency of the number of radial pellet cracks on heat generation rate per unit length – which we show cannot be reproduced by the common assumption in pellet modelling of a deterministic failure strain throughout the pellet volume – was accurately predicted when a size-scaled Weibull distribution with a modulus of 5 was used.
- Crack patterns produced using this 2-dimensional peridynamics method are shown to be similar to other models up to the approximate point in the power history modelled, where such models have been shown to produce accurate crack patterns relative to PIE data after a complete power history. It can therefore be stated with some confidence that the qualitative patterns shown by the 2-dimensional peridynamics method in this work are accurate.

- Using the failure strain of UO_2 as the critical strain for peridynamics bonds produces a nuclear fuel pellet model that first nucleates radial cracks at the expected linear heat rating (~ 5 kW m^{-1}) but without randomisation of bond failure strains, subsequent radial cracks nucleate at lower powers than expected relative to PIE data. Using a Weibull distribution for the failure strains improves the fit, and scaling the distribution to account for the size of the bonds relative to the pellet improves it further.
- Standard UO_2 nuclear fuel pellets are most appropriately modelled using a Weibull modulus, β, of 5-10, although using the method outline in this work necessitates using the higher end of this range to avoid artificial crack nucleation in near-surface regions, which is unphysical. Use of a Weibull modulus of 10 avoided this simulation artefact while still reproducing the experimentally observed dependency with reasonable accuracy.

Credit Author Statement

Lloyd D. Jones

Conceptualization, Methodology, Software, Investigation, Writing - Original Draft, Writing - Review & Editing, Visualization

Thomas A. Haynes

Software, Resources, Writing - Review & Editing, Visualization, Supervision

Glyn Rossiter

Conceptualization, Validation, Writing - Review & Editing, Supervision, Funding acquisition

Mark R. Wenman

Conceptualization, Writing - Review & Editing, Supervision, Project administration, Funding acquisition

Declaration of interests

The authors declare that they have no known competing financial interests or personal relationships that could have appeared to influence the work reported in this paper.

Acknowledgements

Lloyd Jones and Mark Wenman acknowledge support from the Engineering & Physical Sciences Research Council through the Imperial-Cambridge-Open Centre for Doctoral Training, grant number EP/L015900/1, as well as financial support from the UK National Nuclear Laboratory.

Thomas Haynes and Mark Wenman acknowledge support from National Nuclear Laboratory and the UK Department for Business, Energy and Industrial Strategy under the Advanced Fuel Cycle Programme.

References

[1] M. Oguma, "Cracking and relocation behaviour of nuclear fuel pellets during rise to power," *Nuclear Engineering and Design,* vol. 76, pp. 35-45, 1983.

[2] S. Beguin, "PCI-related constraints on EDF PWRs and associated challenges," *Pellet-Clad Interaction in Water Reactor Fuels Transactions, Aix-en-Provence,* pp. 53-62, 2005.

[3] B. Cox, "Pellet-clad interaction (PCI) failures of zirconium alloy fuel cladding - a review," *Journal of Nuclear Materials,* vol. 172, pp. 249-292, 1990.

[4] S. A. Silling, "Reformulation of elasticity theory for discontinuities and long-range forces," *Journal of the Mechanics and Physics of Solids,* vol. 48, 175-209, pp. 175-209, 2000.

[5] S. A. Silling, M. Epton, O. Weckner, J. Xu, and E. Askari, "Peridynamic States and Constitutive Modeling," *Journal of Elasticity,* vol. 88, pp. 151-184, 2007.

[6] H. Huang, B. Spencer, and J. Hales, "Discrete element method for simulation of early-life thermal fracturing behavior in ceramic nuclear fuel pellets," *Nuclear Engineering and Design,* vol. 278, pp. 515-528, 2014, doi: 10.1016/j.nucengdes.2014.05.049.

[7] S. Oterkus and E. Madenci, "Peridynamic Modeling of Fuel Pellet Cracking," *Engineering Fracture Mechanics,* vol. 176, pp. 23-37, 2017.

[8] W. Li and K. Shirvan, "Multiphysics phase-field modeling of quasi-static cracking in urania ceramic nuclear fuel," *Ceramics International,* vol. 47, pp. 793-810, 2021.

[9] A. T. Zehnder, "Griffith Theory of Fracture. ," *Encyclopedia of Tribology*, vol. Springer, Boston (MA), 2013.
[10] L. A. Walton and D. L. Husser, "Fuel Pellet Fracture and Relocation," *Water Reactor Fuel Element Performance Computer Modelling,* pp. 115-152, 1983.
[11] T. Barani, D. Pizzocri, G. Pastore, L. Luzzi, and J. D. Hales, "Isotropic softening model for fuel cracking in BISON," *Nuclear Engineering and Design*, vol. 342, pp. 257–263, 2019.
[12] W. Jiang, B. W. Spencer, and J. E. Dolbow, "Ceramic nuclear fuel fracture modeling with the extended finite element method," *Engineering Fracture Mechanics*, vol. 223, 2020, Art no. 1067132.
[13] Y. Wang, X. Zhou, and M. Kou, "Peridynamic investigation on thermal fracturing behavior of ceramic nuclear fuel pellets under power cycles," *Ceramics International,* vol. 44, pp. 11512-11542, 2018.
[14] R. Mella and M. R. Wenman, "Modelling explicit fracture of nuclear fuel pellets using peridynamics," *Journal of Nuclear Materials,* vol. 467, pp. 58-67, 2015, doi: 10.1016/j.jnucmat.2015.08.037.
[15] R. Mella, "Finite Element Modelling of the Advanced Gas-Cooled Reactor Fuel Performance," *PhD Thesis, Imperial College London,* 2014.
[16] Y. Hu, H. Chen, B. Spencer, and E. Madenci, "Thermomechanical peridynamic analysis with irregular non-uniform domain discretization," *Engineering Fracture Mechanics*, vol. 197, pp. 92-113, 2018.
[17] S. Guo *et al.*, "Statistical Analysis on the Mechanical Properties of Magnesium Alloys," *Materials,* vol. 10, pp. 1271-1278, 2017.
[18] L. D. Jones, L. J. Vandeperre, T. A. Haynes, and M. R. Wenman, "Theory and Application of Weibull Distributions to 1D Peridynamics for Brittle Solids," *Computer Methods in Applied Mechanics and Engineering*, vol. 363, 2020, Art no. 112903.
[19] L. D. Jones, L. J. Vandeperre, T. A. Haynes, and M. R. Wenman, "Modelling of Weibull Distributions in Brittle Solids Using 2-Dimensional Peridynamics," *Structural Integrity Procedia*, vol. 28, pp. 1856–1874, 2020.
[20] O. E. Strack, R. B. Leavy, and R. M. Brannon, "Aleatory uncertainty and scale effects in computational damage models for failure and fragmentation," *International Journal for Numerical Methods In Engineering,* vol. 102, pp. 468-495, 2015.
[21] R. W. Macek and S. A. Silling, "Peridynamics via finite element analysis," *Finite Elements in Analysis and Design,* vol. 43, no. 15, pp. 1169-1178, 2007, doi: 10.1016/j.finel.2007.08.012.
[22] A. Bamgboye, T. A. Haynes, and M. R. Wenman, "Predicting crack patterns in SiC-based cladding for LWR applications using peridynamics," *Structural Integrity Procedia,* vol. 28, pp. 1520–1535, 2020.

[23] T. A. Haynes, D. Shepherd, and M. R. Wenman, "Preliminary Modelling of Crack Formation and Propagation in SiC / SiC Accident-Tolerant Fuel during Routine Operational Transients using Peridynamics," *Journal of Nuclear Materials,* vol. 540, 2020, Art no. 152369.

[24] R. Beckmann, R. Mella, and M. R. Wenman, "Mesh and timestep sensitivity of fracture from thermal strains using peridynamics implemented in Abaqus," *Computer Methods in Applied Mechanics and Engineering,* vol. 263, pp. 71-80, 2013, doi: 10.1016/j.cma.2013.05.001.

[25] Y. D. Ha and F. Bobaru, "Studies of dynamic crack propagation and crack branching with peridynamics," *International Journal of Fracture,* vol. 162, pp. 229–244, 2010.

[26] Y. D. Ha and F. Bobaru, "Characteristics of dynamic brittle fracture captured with peridynamics," *Engineering Fracture Mechanics,* vol. 78, no. 6, pp. 1156-1168, 2011.

[27] G. Rossiter, "Development of the ENIGMA fuel performance code for whole core analysis and dry storage assessments," *Nuclear engineering and Technology,* vol. 43, no. 6, pp. 489-498, 2011.

[28] L. J. Siefken, E. W. Coryell, E. A. Harvego, and J. K. Hohorst, "MATPRO - A Library of Materials Properties for Light-Water-Reactor Accident Analysis," *Idaho National Engineering and Environmental Laboratory,* 2001.

[29] M. Oguma, "Microstructure Effects on Fracture Strength of UO_2 Fuel Pellets," *Journal of Nuclear Science and Technology,* vol. 19, no. 12, pp. 1005-1014, 1982.

[30] K. C. Radford, "Effect of fabrication parameters and microstructure on the mechanical strength of UO_2 fuel pellets," *Journal of Nuclear Materials,* vol. 84, no. 1-2, pp. 222-236, 1979.

[31] A. A. Griffiths, "The Phenomena of Rupture and Flow in Solids," *Philosophical Transactions of the Royal Society of London. Series A, Containing Papers of a Mathematical or Physical Character,* vol. 221, pp. 163-198, 1921.

[32] C. Ruggieri and A. P. Jivkov, "A probabilistic approach for cleavage fracture including the statistics ofmicrocracks: Application to a reactor pressure vessel steel," *Engineering Fracture Mechanics,* vol. 272, 2022, Art no. 108702.

[33] T. A. Haynes, J. A. Ball, and M. R. Wenman, "Modelling the Role of Pellet Relocation in the (r-θ) Plane Upon Pellet-Clad Interaction in Advanced Gas Reactor Fuel," *Nuclear Engineering & Design,* vol. 314, pp. 271-284, 2017.

[34] W. E. Pennell and W. R. Corwin, "Reactor Pressure Vessel Structural Integrity Research In the U.S Nuclear Regulatory Commission HSSTand HSSI Programs," *Oak Ridge National Laboratory,* vol. TI95011768, 1994.

[35] L. J. Vandeperre, A. Kristofferson, E. Carlstrom, and W. J. Clegg, "Thermal Shock of Layered Ceramic Structures with Crack-Deflecting Interfaces," *Journal of the American Ceramic Society*, vol. 84, no. 1, pp. 104-110, 2001.

[36] B. Michel, J. Sercombe, G. Thouvenin, and R. Chatelet, "3D fuel cracking modelling in pellet cladding mechanical interaction," *Engineering Fracture Mechanics*, vol. 75, no. 11, pp. 3581-3598, 2008, doi: 10.1016/j.engfracmech.2006.12.014.

[37] K. A. Gamble, T. W. Knight, E. Roberts, J. D. Hales, and B. W. Spencer, "Mechanistic verification of empirical UO_2 fuel fracture models," *Journal of Nuclear Materials*, vol. 556, 2021, Art no. 153163.

[38] B. W. Spencer *et al.*, "Dry in-pile fracture test (DRIFT) for separate-effects validation of ceramic fuel fracture models," *Journal of Nuclear Materials*, vol. 568, 2022, Art no. 153816.

[39] S. Patnaik, B. W. Spencer, E. Roberts, T. M. Besmann, and T. W. Knight, "Separate-Effects Tests for Studying TemperatureGradient-Driven Cracking in UO_2 Pellets," *Nuclear Science and Engineering*, vol. 195, no. 12, pp. 1307-1326, 2021.